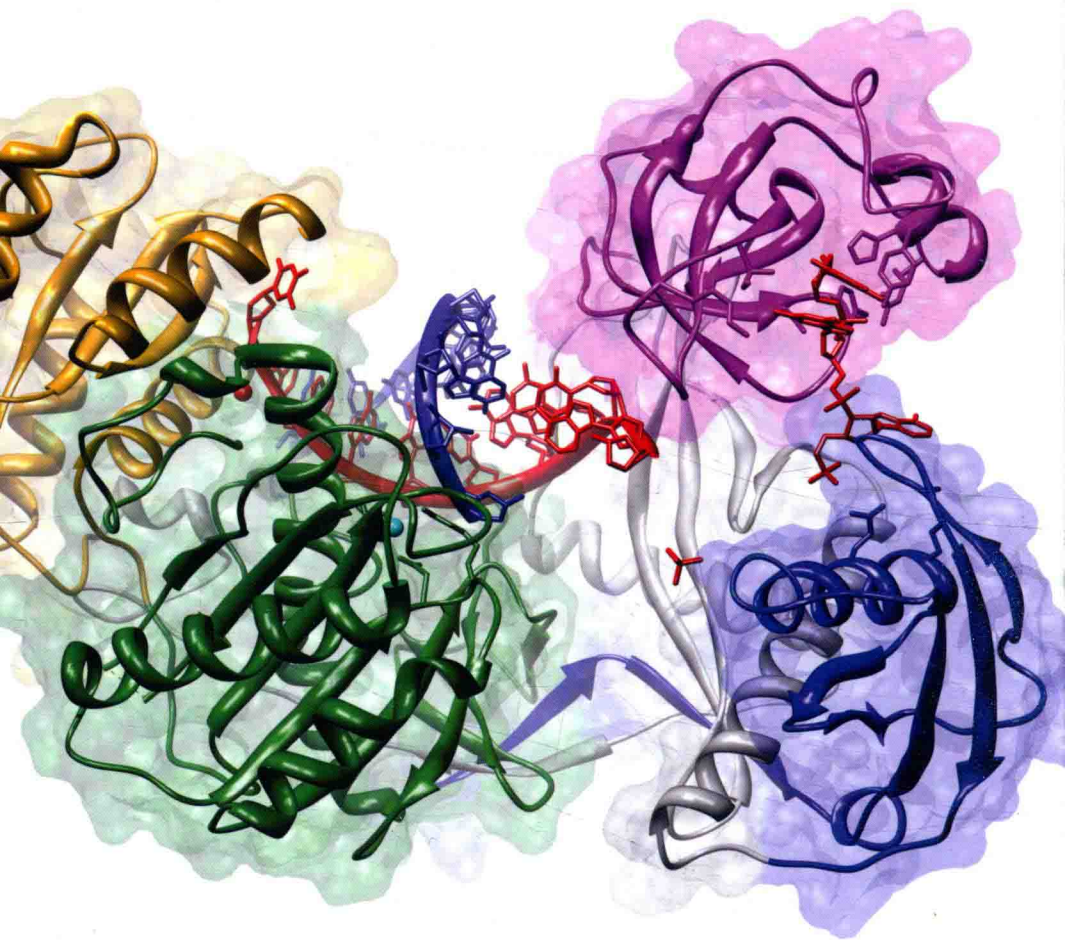


Protein Interactions

Research and Development



Anton Torres

Protein Interactions: Research and Development

Edited by Anton Torres



New York

Published by Callisto Reference,
106 Park Avenue, Suite 200,
New York, NY 10016, USA
www.callistoreference.com

Protein Interactions: Research and Development

Edited by Anton Torres

© 2015 Callisto Reference

International Standard Book Number: 978-1-63239-520-7 (Hardback)

This book contains information obtained from authentic and highly regarded sources. Copyright for all individual chapters remain with the respective authors as indicated. A wide variety of references are listed. Permission and sources are indicated; for detailed attributions, please refer to the permissions page. Reasonable efforts have been made to publish reliable data and information, but the authors, editors and publisher cannot assume any responsibility for the validity of all materials or the consequences of their use.

The publisher's policy is to use permanent paper from mills that operate a sustainable forestry policy. Furthermore, the publisher ensures that the text paper and cover boards used have met acceptable environmental accreditation standards.

Trademark Notice: Registered trademark of products or corporate names are used only for explanation and identification without intent to infringe.

Printed in China.

Preface

This book, written by renowned experts, provides advanced researches and concepts in the field of protein interactions. The book presents the interaction between proteins and other biomolecules, which is crucial to all features of biological procedures such as cell growth and differentiation. Hence, examination and modulation of protein interactions are of vital importance, as it not only discloses the mechanism governing cellular movement, but also leads to possible agents for the treatment of a broad range of disorders. The purpose of this book is to emphasize some of the most recent advances in the study of protein interactions, along with modulation of protein interactions, improvements in systematic methods, etc. It provides various examples of protein interaction as the book demonstrates the significance and the opportunities for further exploration of protein interactions.

This book is a result of research of several months to collate the most relevant data in the field.

When I was approached with the idea of this book and the proposal to edit it, I was overwhelmed. It gave me an opportunity to reach out to all those who share a common interest with me in this field. I had 3 main parameters for editing this text:

1. Accuracy - The data and information provided in this book should be up-to-date and valuable to the readers.
2. Structure - The data must be presented in a structured format for easy understanding and better grasping of the readers.
3. Universal Approach - This book not only targets students but also experts and innovators in the field, thus my aim was to present topics which are of use to all.

Thus, it took me a couple of months to finish the editing of this book.

I would like to make a special mention of my publisher who considered me worthy of this opportunity and also supported me throughout the editing process. I would also like to thank the editing team at the back-end who extended their help whenever required.

Editor

Contents

	Preface	VII
	Examples of Protein Interactions	1
Chapter 1	Autophagy-Mediated Defense Response of Mouse Mesenchymal Stromal Cells (MSCs) to Challenge with <i>Escherichia coli</i> N.V. Gorbunov, B.R. Garrison, M. Zhai, D.P. McDaniel, G.D. Ledney, T.B. Elliott and J.G. Kiang	3
Chapter 2	MOZ-TIF2 Fusion Protein Binds to Histone Chaperon Proteins CAF-1A and ASF1B Through Its MOZ Portion Hong Yin, Jonathan Glass and Kerry L. Blanchard	25
Chapter 3	The Use of Reductive Methylation of Lysine Residues to Study Protein-Protein Interactions in High Molecular Weight Complexes by Solution NMR Youngshim Lee, Sherwin J. Abraham and Vadim Gaponenko	45
Chapter 4	Regulation of Protein-Protein Interactions by the SUMO and Ubiquitin Pathways Yifat Yanku and Amir Orian	53
Chapter 5	The TPR Motif as a Protein Interaction Module - A Discussion of Structure and Function Natalie Zeytuni and Raz Zarivach	71
Chapter 6	Functional Protein Interactions in Steroid Receptor-Chaperone Complexes Thomas Ratajczak, Rudi K. Allan, Carmel Cluning and Bryan K. Ward	87
Chapter 7	Protein-Protein Interactions and Disease Aditya Rao, Gopalakrishnan Bulusu, Rajgopal Srinivasan and Thomas Joseph	119

Chapter 8	Direct Visualization of Single-Molecule DNA-Binding Proteins Along DNA to Understand DNA-Protein Interactions Hiroaki Yokota	131
Chapter 9	Defining the Cellular Interactome of Disease-Linked Proteins in Neurodegeneration Verena Arndt and Ina Vorberg	151
Chapter 10	Protein Interactions in S-RNase-Based Gametophytic Self-Incompatibility Thomas L. Sims	179
Chapter 11	Biochemical, Structural and Pathophysiological Aspects of Prorenin and (Pro)renin Receptor A.H.M. Nurun Nabi and Fumiaki Suzuki	203
Chapter 12	Cholesterol-Binding Peptides and Phagocytosis Antonina Dunina-Barkovskaya	235

Permissions

List of Contributors

Examples of Protein Interactions

Autophagy-Mediated Defense Response of Mouse Mesenchymal Stromal Cells (MSCs) to Challenge with *Escherichia coli*

N.V. Gorbunov^{1,*}, B.R. Garrison¹, M. Zhai¹, D.P. McDaniel²,
G.D. Ledney³, T.B. Elliott³ and J.G. Kiang^{3,*}

¹The Henry M. Jackson Foundation for the Advancement of Military Medicine, Inc.

²The Department of Microbiology and Immunology, School of Medicine,

³Radiation Combined Injury Program, Armed Forces Radiobiology Research Institute,
Uniformed Services University of the Health Sciences, Bethesda, Maryland,
USA

1. Introduction

Symbiotic microorganisms are spatially separated from their animal host, e.g., in the intestine and skin, in a manner enabling nutrient metabolism as well as evolutionary development of protective physiologic features in the host such as innate and adaptive immunity, immune tolerance, and function of tissue barriers (1,2). The major interface barrier between the microbiota and host tissue is constituted by epithelium, reticuloendothelial tissue, and mucosa-associated lymphoid tissue (MALT) (2,3).

Traumatic damage to skin and the internal epithelium in soft tissues can cause infections that account for 7% to 10% of hospitalizations in the United States (4). Moreover, wound infections and sepsis are an increasing cause of death in severely ill patients, especially those with immunosuppression due to exposure to cytotoxic agents and chronic inflammation (4). It is well accepted that breakdown of the host-bacterial symbiotic homeostasis and associated infections are the major consequences of impairment of the "first line" of antimicrobial defense barriers such as the mucosal layers, MALT and reticuloendothelium (1-3). Under these impairment conditions of particular interest then is the role of sub-mucosal structures, such as connective tissue stroma, in the innate defense compensatory responses to infections.

The mesenchymal connective tissue of different origins is a major source of multipotent mesenchymal stromal cells (i.e., colony-forming-unit fibroblasts) (5, 6). Recent discovery of immunomodulatory function of mesenchymal stromal cells (MSCs) suggests that they are essential constituents that control inflammatory responses (6-7).

Recent *in vivo* experiments demonstrate promising results of MSC transfusion for treatment of acute sepsis and penetrating wounds (7-9). The molecular mechanisms underlying MSC

* Corresponding Authors

action in septic conditions are currently under investigation. It is known to date that (i) Gram-negative bacteria can induce an inflammatory response in MSCs *via* cascades of Toll-like receptor (type 4) and the nucleotide-binding oligomerization domain-containing protein 2 (NOD2) complexes recognizing the conserved pathogen-associated molecular patterns; (ii) activated MSCs can modulate the septic response of resident myeloid cells; and (iii) activated MSCs can directly suppress bacterial proliferation by releasing antimicrobial factors (10, 11).

Considering all of the above factors including the fact that MSCs are ubiquitously present in the sub-mucosal structures and conjunctive tissue, one would expect involvement of these cells in formation of antibacterial barriers and host-microbiota homeostasis. From this perspective our attention was attracted by the phagocytic properties of mesenchymal fibroblastic stromal cells documented in an early period of their investigation (5, 12). The phagocytosis mechanism is closely and synchronously connected with the cellular mechanisms of biodegradation mediated by the macroautophagy-lysosomal (autolysosomal) system (13-15). The last one decomposes proteins and organelles as well as bacteria and viruses inside cells and, therefore, is considered as a part of the innate defense mechanism (13- 15).

Macroautophagy (hereafter referred to as autophagy) is a catabolic process of bulk lysosomal degradation of cell constituents and phagocytized particles (16). Autophagy dynamics in mammalian cells are well described in recent reviews (14, 17-20). Thus, it was proposed that autophagy is initiated by the formation of the phagophore, followed by a series of steps, including the elongation and expansion of the phagophore, closure and completion of a double-membrane autophagosome (which surrounds a portion of the cytoplasm), autophagosome maturation through docking and fusion with an endosome (the product of fusion is defined as an amphisome) and/or lysosome (the product of fusion is defined as an autolysosome), breakdown and degradation of the autophagosome inner membrane and cargo through acid hydrolases inside the autolysosome, and recycling of the resulting macromolecules through permeases (14). These processes, along with the drastic membrane traffic, are mediated by factors known as autophagy-related proteins (i.e., ATG-proteins) and the lysosome-associated membrane proteins (LAMPs) that are conserved in evolution (21). The autophagic pathway is complex. To date there are over 30 ATG genes identified in mammalian cells as regulators of various steps of autophagy, e.g., cargo recognition, autophagosome formation, etc. (14, 22). The core molecular machinery is comprised of (i) components of signaling cascades, such as the ULK1 and ULK2 complexes and class III PtdIns3K complexes, (ii) autophagy membrane processing components, such as mammalian Atg9 (mAtg9) that contributes to the delivery of membrane to the autophagosome as it forms, and two conjugation systems: the microtubule-associated protein 1 (MAP1) light chain 3 (i.e., LC3) and the Atg12-Atg5-Atg16L complex. The two conjugation systems are proposed to function during elongation and expansion of the phagophore membrane (14, 19, 22, 23). A conservative estimate of the autophagy network counts over 400 proteins, which, besides the ATG-proteins, also include stress-response factors, cargo adaptors, and chaperones such as p62/SQSTM1 and heat shock protein 70 (HSP70) (15, 19, 22, 24, 26-28).

Autophagy is considered as a cytoprotective process leading to tissue remodeling, recovery, and rejuvenation. However, under circumstances leading to mis-regulation of the

autolysosomal pathway, autophagy can eventually cause cell death, either as a precursor of apoptosis in apoptosis-sensitive cells or as a result of destructive self-digestion (29).

Based on this information we hypothesized that challenge of MSCs with *Escherichia coli* (*E. coli*) can induce a complex process where bacterial phagocytosis is accompanied by activation of autolysosomal pathway and stress-adaptive responses in MSCs. The objective of this current chapter is to provide evidence of this hypothesis.

2. Hypothesis test: Experimental procedures and technical approach

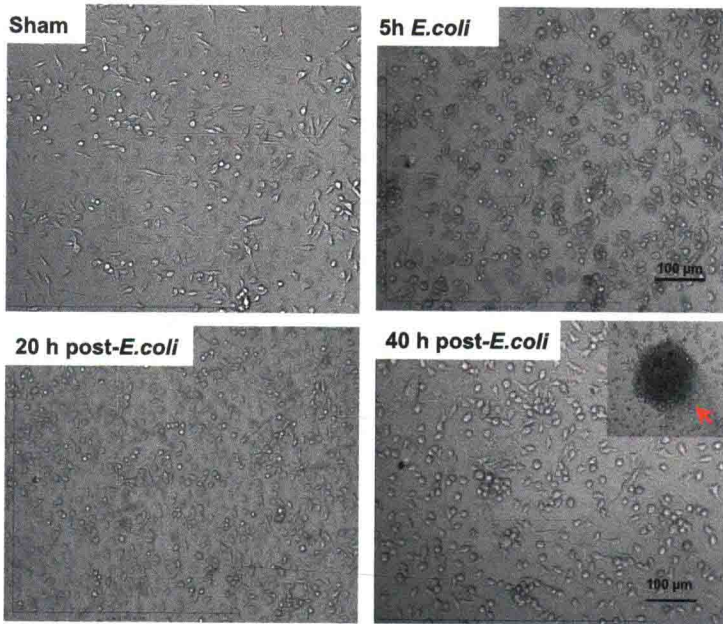
2.1 Bone marrow stromal cells

Bone marrow stromal cells were obtained from 3- to 4-month-old B6D2F1/J female mice using a protocol adapted from STEMCELL Technologies, Inc., and were expanded and cultivated in hypoxic conditions (5% O₂, 10% CO₂, 85% N₂) for approximately 30 days in MESENCULT medium (STEMCELL Technologies, Inc.) in the presence of antibiotics. Phenotype, proliferative activity, and colony-forming ability of the cells were analyzed by flow cytometry and immunofluorescence imaging using positive markers for mesenchymal stromal cells: CD44, CD105, and Sca1. The results of these analyses showed that the cultivated cells displayed properties of mesenchymal stromal clonogenic fibroblasts.

The experiments were performed in a facility accredited by the Association for the Assessment and Accreditation of Laboratory Animal Care-International (AAALAC-I). All animals used in this study received humane care in compliance with the Animal Welfare Act and other federal statutes and regulations relating to animals and experiments involving animals and adhered to principles stated in the Guide for the Care and Use of Laboratory Animals, NRC Publication, 1996 edition.

2.2 Challenge of MSCs with *Escherichia coli* bacteria

MSC cultures of approximate 80% confluency were challenged with proliferating *E. coli* (1×10^7 microorganisms/ml) for 1-5 h in antibiotic-free media. For assessment of the cellular alteration ≥ 5 h the incubation medium was replaced with fresh medium containing penicillin and streptavidin antibiotics. Bacteria-cell interaction was monitored with time-lapse microscopy using DIC imaging of MSCs and fluorescence imaging of *E. coli* labeled with PSVue® 480, a fluorescent cell tracking reagent (www.mtarget.com). At the end of the experiments the cells were either (i) harvested, washed, and lysed for qRT-PCR and immunoblot analyses, (ii) fixed for transmission electron microscopy and fluorescence confocal imaging, or (iii) used live for imaging of Annexin V reactivity, dihydrorhodamine 123, a sensitive indicator of peroxynitrite reactivity, and colony formation. With this protocol the cells were tested for (i) phagocytic activity; (ii) autolysosomal activity; (iii) production of reactive oxygen (ROS) and nitrogen species, (iii) stress responses to *E. coli*; (iv) genomic DNA damage and pro-apoptotic alterations; and (v) colony-forming ability. The results of observations indicated that challenge with *E. coli* did not diminish viability and colony forming ability of the cells under the selected conditions (Fig.1). Stimulation of MSCs with *E. coli* resulted in expression of the proinflammatory genes, IL-1 α , IL-1 β , IL-6, and iNOS, as determined with qRT-PCR analysis.



Conditions: MSCs were incubated with $\sim 1 \times 10^7$ /ml *E. coli* for 5 h in medium (without antibiotics). After 5 h the medium was replaced with fresh medium (with antibiotics) and MSCs were incubated for another 40 h. Inset: formation of colonies (red arrowhead) occurred at 72 h post-exposure to *E. coli*.

Fig. 1. Bright field microscopy of MSCs challenged with *E. coli*. Images presented in the panels are MSCs at different time-points following exposure of MSCs to *E. coli*.

2.3 Analysis of the cell proteins

Proteins from MSCs were extracted in accordance with the protocol described previously (30). The aliquoted proteins (20 μ g total protein per gel well) were separated on SDS-polyacrylamide slab gels (NuPAGE 4-12% Bis-Tris; Invitrogen, Carlsbad, CA). After electrophoresis, proteins were blotted onto a PDVF membrane and the blots were incubated with antibodies (1 μ g/ml) raised against MAP LC3, Lamp-1, p62/SQSTM1, p65(NF κ B), Nrf2, HSP70, iNOS, and actin (Abcam, Santa Cruz Biotechnology Inc., LifeSpan Biosciences, Inc., eBiosciences) followed by incubation with species-specific IgG peroxidase conjugate. IgG amounts did not alter after radiation. IgG, therefore, was used as a control for protein loading.

2.4 Immunofluorescent staining and image analysis

MSCs (5 specimens per group) were fixed in 2% paraformaldehyde and analyzed with fluorescence confocal microscopy following labeling (30). Normal donkey serum and antibody were diluted in phosphate-buffered saline (PBS) containing 0.5% BSA and 0.15% glycine. Any nonspecific binding was blocked by incubating the samples with purified normal donkey serum (Santa Cruz Biotechnology, Inc., Santa Cruz, CA) diluted 1:20. Primary antibodies were raised against MAP LC3, Lamp-1, p62/SQSTM1, p65(NF κ B),

Nrf2, Tom 20, and iNOS. That was followed by incubation with secondary fluorochrome-conjugated antibody and/or streptavidin-AlexaFluor 610 conjugate (Molecular Probes, Inc., Eugene OR), and with Hoechst 33342 (Molecular Probes, Inc., Eugene OR) diluted 1:3000. Secondary antibodies used were AlexaFluor 488 and AlexaFluor 594 conjugated donkey IgG (Molecular Probes Inc., Eugene OR). Negative controls for nonspecific binding included normal goat serum without primary antibody or with secondary antibody alone. Five confocal fluorescence and DIC images of crypts (per specimen) were captured with a Zeiss LSM 7100 confocal microscope. The immunofluorescence image analysis was conducted as described previously (30).

2.5 Transmission Electron Microscopy (TEM)

MSCs in cultures were fixed in 4% formaldehyde and 4% glutaraldehyde in PBS overnight, post-fixed in 2% osmium tetroxide in PBS, dehydrated in a graduated series of ethanol solutions, and embedded in Spurr's epoxy resin. Blocks were processed as described previously (30). The sections of embedded specimens were analyzed with a Philips CM100 electron microscope.

2.6 RNA isolation and qRT-PCR

Total cellular RNA was isolated from MSC pellets using the Qiagen RNeasy miniprep kit, quantified by measuring the absorbance at 260nm on a Nanodrop, and qualified by electrophoresis on a 1.2% agarose gel. cDNA was synthesized using Superscript II (Invitrogen) and qRT-PCR was performed using SYBR Green iQ Supermix (Bio-Rad), each according to the manufacturers' instructions. The quality of qRT-PCR data were verified by melt curve analysis, efficiency determination, agarose gel electrophoresis, and sequencing. Relative gene expression was calculated by the method of Pfaffl using the formula $2^{-\Delta\Delta Ct}$ (31).

2.7 Statistical analysis

Statistical significance was determined using one-way ANOVA followed by post-hoc analysis with pair-wise comparison by Tukey-Kramer test. Significance is reported at a level of $p < 0.05$.

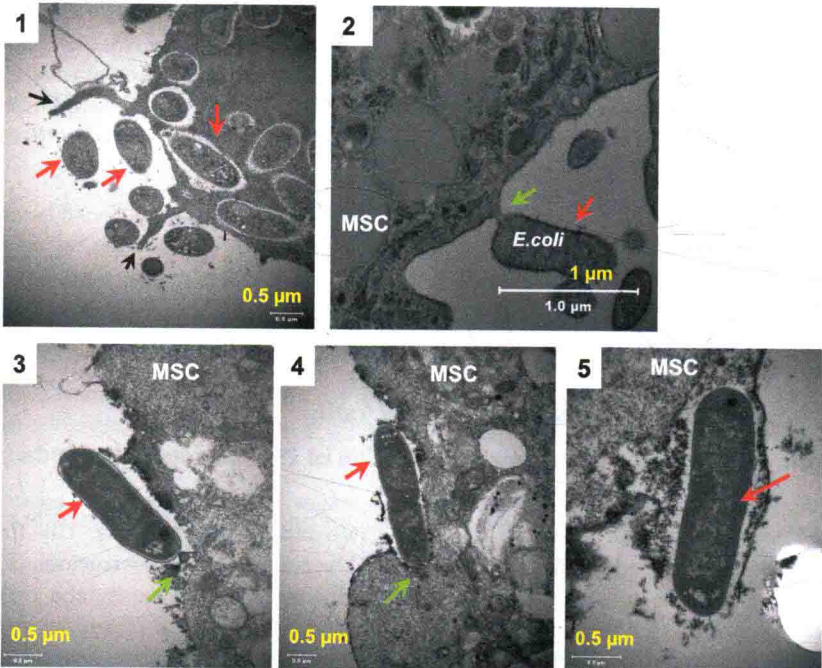
3. Response of MSCs to challenge with *E. coli*

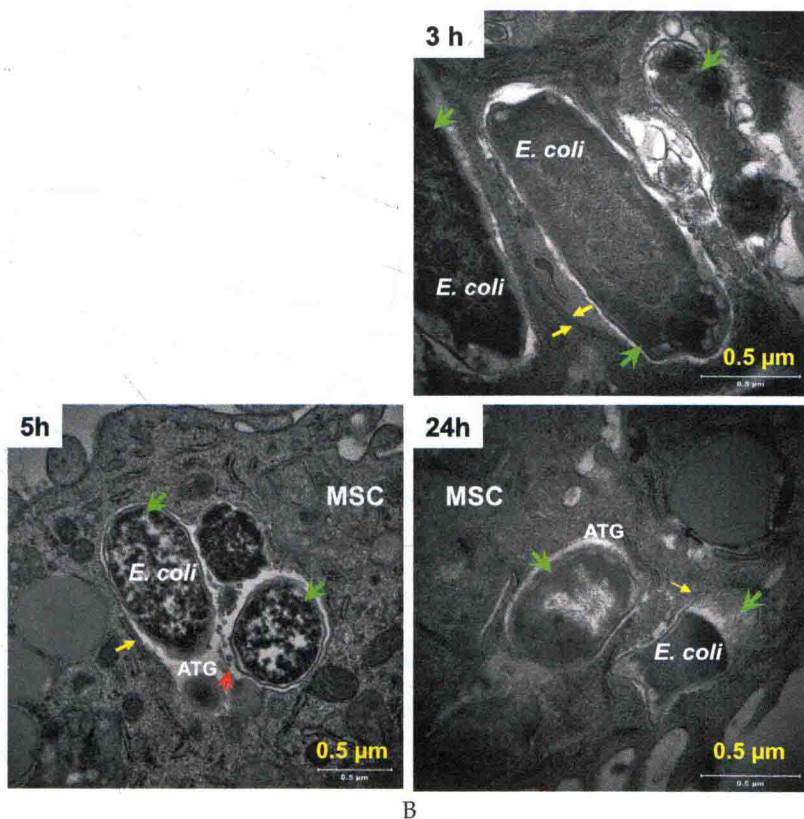
3.1 Phagocytosis and autolysosomal degradation of *E. coli* bacteria by MSCs

TEM images presented in Fig. 2 show different stages of cell-bacterium interaction. The uptake of microorganisms occurred in at least two independent events. The first event encompassed engulfing and taking in particles by the cell membrane extrusions (Fig. 2A1). The second event was tethering and "zipping" of adhered particles by the cell plasma membrane (Fig. 2A2 - 2A5). The time-lapse fluorescence microscopy observation indicated that these events proceeded quickly and the uptake process required a few minutes (not shown). Thereafter, a significant amount of bacteria in MSCs was observed within 1 h of co-incubation of the cells. The phagocytized bacteria were subjected to autolysosomal

degradation (Fig 2B). Formation of the double-membrane autophagosomes, which incorporated bacteria, was observable in MSCs at 3 h of co-incubation and during a further period of observation. Fusion of autophagosomes with lysosomes also occurred at this period. Fragmentation of bacterial constituents was observed at 5 h of co-incubation and appearance of bacterial “ghosts” at 24 h (Fig. 2B).

Various cells eliminate bacterial microorganisms by autophagy, and this elimination is in many cases crucial for host resistance to bacterial translocation. Although autophagy is a non-selective degradation process, autophagosomes do not form randomly in the cytoplasm, but rather sequester the bacteria selectively (32, 33). Therefore, autophagosomes that engulf microbes are sometimes much larger than those formed during degradation of cellular organelles, suggesting that the elongation step of the autophagosome membrane is involved in bacteria-surrounding autophagy (33). The mechanism underlying selective induction of autophagy at the site of microbe phagocytosis remains unknown. However, it is likely mediated by pattern recognition receptors, stress-response elements, and adaptor proteins, e.g., p62/SQSTM1, which target bacteria and ultimately recruit factors essential for formation of autophagosomes (13,14, 33, 34).





B

Conditions: MSCs were incubated with $\sim 1 \times 10^7$ /ml *E. coli* either for 3 h or 5 h in MesenCult Medium (without antibiotics). After 5 h the medium was replaced with fresh medium (with antibiotics) and MSCs were incubated for another 19 h.

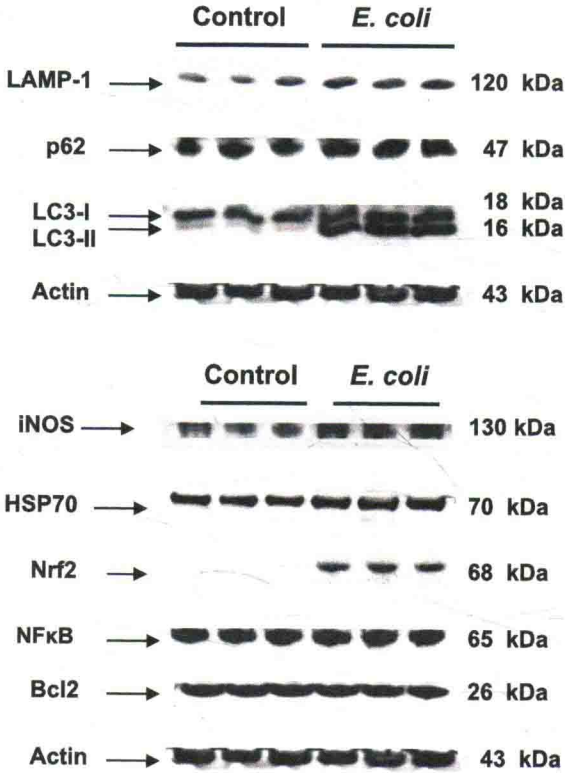
Fig. 2. Transmission electron micrographs (TEM) of *E. coli* phagocytosis by MSCs and autolysosomal degradation of phagocytized bacteria.

A) Panel A1: Engulfing and up-take of bacteria (red arrows) by the cell plasma membrane extrusions (black arrows). Panels A2-A5: Tethering and zipping (green arrows) and up-take of bacteria (red arrows) by the cell plasma membrane. Specimens were fixed at 3 h co-incubation of MSCs with bacteria.

B) Autolysosomal degradation of phagocytized bacteria at different time-points after exposure of MSCs to *E. coli* (green arrows). Autophagosome (ATG) membranes are indicated with yellow arrows. Lysosome fusion with autophagosomes is indicated with red arrows.

The results of TEM were corroborated by the data obtained with immunoblotting and immunofluorescence confocal imaging of autophagy MAP (LC3) protein, lysosomal LAMP1 and the ubiquitin-associated target adaptor p62. A key step in the autophagosome biogenesis is the conversion of light-chain protein 3 type I (LC3-I, also known as ubiquitin-like protein, Atg8) to type II (LC3-II). The conversion occurs via the cleavage of the LC3-I carboxyl terminus by a redox-sensitive Atg4 cysteine protease. The subsequent binding of

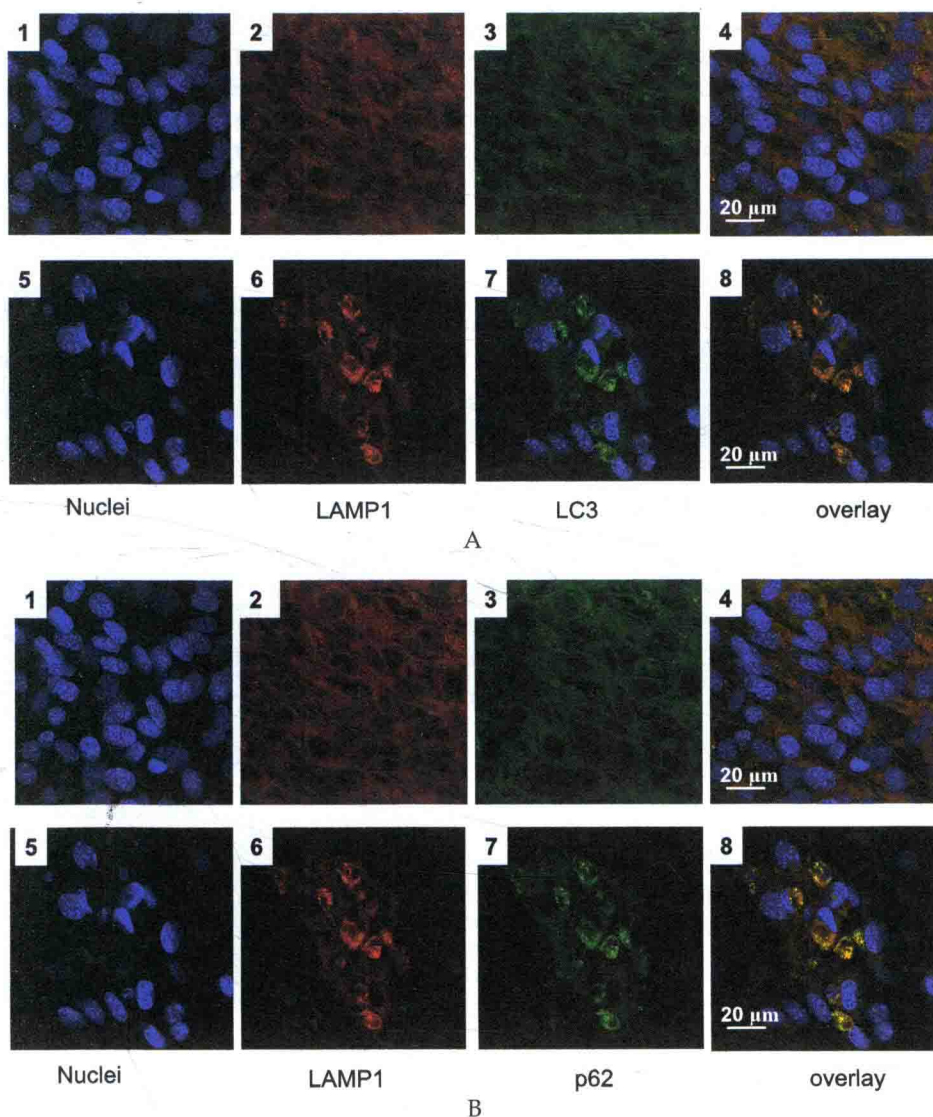
the modified LC3-I to phosphatidylethanolamine, i.e., process of lipidation of LC3-I, on the isolation membrane, as it forms, is mediated by E-1- and E-2-like enzymes Atg7 and Atg3 (14). Therefore, conversion of LC3-I to LC3-II and formation of LC3-positive vesicles are considered to be a marker of activation of autophagy (14). A growing body of evidence suggests involvement of chaperone HSP70 in regulation of LC3-translocation. The results of immunoblot analysis of the proteins indicated an increase in the LC3-I to LC3-II - transition in the *E. coli*-challenged MSCs (Fig. 3).



Conditions: MSCs were incubated with $\sim 1 \times 10^7$ /ml *E. coli* for 3 h in MesenCult Medium (without antibiotics). After 3 h the medium was replaced with fresh medium (with antibiotics) and MSCs were further incubated for another 21 h.

Fig. 3. Immunoblotting analysis of LC3, LAMP1 autolysosomal proteins, p62 adaptor protein, and stress-response elements: NF- κ B(p65), Nrf2, HSP70 in MSCs challenged with *E. coli*.

The images presented in Fig. 4A indicate an increase of formation of LC3-positive vesicles in MSCs challenged with *E. coli*. The LC3 immunoreactivity co-localized with immunoreactivity to LAMP1, a marker of lysosomes, indicating presence of fusion of autophagosomes with lysosomes, i.e., formation of autolysosomes (Fig. 4A). This effect



Conditions: MSCs were incubated with $\sim 1 \times 10^7$ /ml *E. coli* for 3 h in MesenCult Medium (without antibiotics). After 3 h the medium was replaced with fresh medium (with antibiotics) and MSCs were further incubated for 21 h. Projections of LAMP1 protein (red channel) are shown in panels A2, A6, B2, and B6. Projections of LC3 protein (green channel) are shown in panels A3 and A7. Projections of p62 protein (green channel) are shown in panels B3 and B7. Counterstaining of nuclei was with Hoechst 33342 (blue channel). Panels A4, A8, B4, and B8 are overlay of signals acquired in the red, green, and blue channels. The confocal images were taken with pinhole setup to obtain 0.5 μm Z-sections.

Fig. 4. Immunofluorescence confocal imaging of the LC3, LAMP1, and p62 protein in MSCs challenged with *E. coli*. Panels A1-A4 and B1-B4 are control specimens. Panels A5-A8 and B5-B8 are challenged with *E. coli*.